Electronic Supplementary Information

Custom designed nanocrystalline Li_2MSiO_4/reduced graphene oxide (M=Fe, Mn) formulations as high capacity cathodes for rechargeable lithium batteries

D. Bhuvaneswari[a], N. Kalaiselvi[*,a]

[a]- ECPS Division, CSIR-Central Electrochemical Research Institute, Karaikudi-630006, India.

Fax: +91 04565-227779

E-mail: kalaiselvicecri@gmail.com

1. Synthesis of rGO and Li_2MSiO_4/ rGO Nanocomposites

Primarily, 1g of graphite flakes were chemically oxidized by treatment with 50 ml of 98% H_2SO_4, 3g of $KMnO_4$1g of $NaNO_3$and 30% H_2O_2wereadded to complete the reaction. The product was washed by 3% HCl in order to remove Mn^{2+} and SO_4^{2-}followed by mixed aqueous solution of 3%H_2SO_4 and 0.5% H_2O_2 to eliminate other impurities and centrifuged. Further, washing was continued with water until neutral pH is realized. Finally, the residue was dried in vacuum oven at overnight to remove the moisture content. The resultant product isgraphite oxide. Subsequently, graphite oxide was diluted with water and subjected to mild sonication for longer time followed by centrifugation, during which the supernatant liquid viz., graphene oxide(GO) was collected carefully. Further, chemical reduction of graphene oxide (GO) was carried out by treating the same with hydrazine hydrate. The contents upon heating in an oil bath at 100 °C for 24h form the precipitate of reduced GO(rGO),which appears as a black solid.In the present study, 500 mg of ortho silicate active material was added directly to GO solution and reduced with hydrazine hydrate to get in-situ reduced Li_2MSiO_4/rGO. The nanocomposites of Li_2MSiO_4/CNT were obtained by mixing the native silicate powders individually with CNT (10

wt%) and ballmilled for 2h to obtain the homogeneous distribution of CNT upon cathode active material.

2. Synthesis of Li_2FeSiO_4 and Li_2MnSiO_4 by sol-gel method

Li_2MnSiO_4 nanoparticles were synthesized from the starting materials of $LiCH_3COO$ (Sigma-Aldrich), SiO_2(Sigma-Aldrich), $Mn(CH_3COO)_2$(Sigma-Aldrich) and citric acid (Sigma-Aldrich) using a conventional sol–gelmethod. A stoichiometric amount of each material was dissolved in water and mixed well with an aqueous solution of 1M citric acid (as a chelating agent. The mixture was evaporated at 90 °C to form a transparent sol. Then, the sol was transferred to vacuum oven and dried at 110 °C to obtain the dried products. The procedure was adoted for Li_2FeSiO_4 synthesis with the starting materials of $LiCH_3COO$ (Sigma-Aldrich), SiO_2(Sigma-Aldrich), $Fe(C_2O_4)$ (Sigma-Aldrich) and citric acid (Sigma-Aldrich). The resulting precursor was finely ground and calcined at 700 °C for 5h in Ar atmosphere to yield the final powder product.

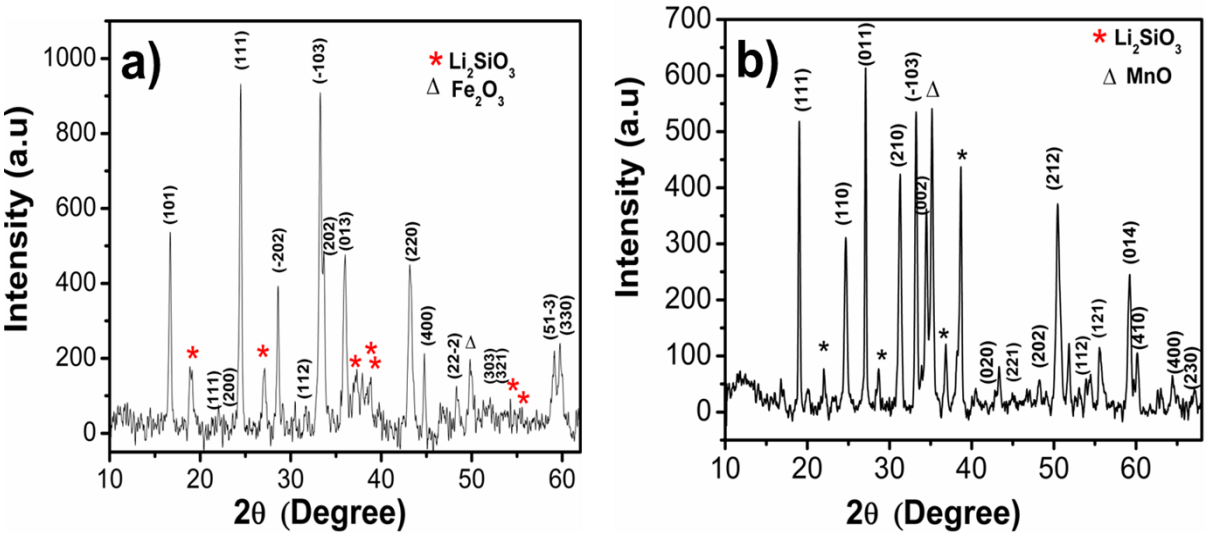

Fig. S1. XRD pattern of sol-gel synthesized (a) Li_2FeSiO_4 and (b) Li_2MnSiO_4

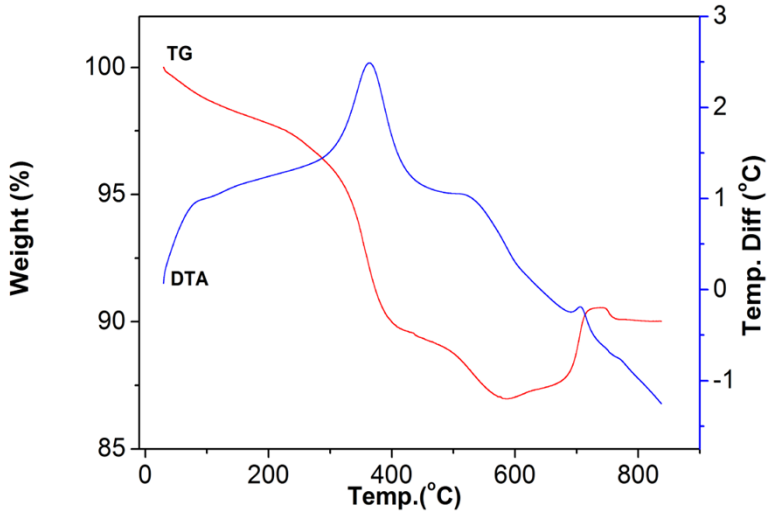

Fig. S2. Typical TG-DTA behavior of Li_2FeSiO_4/rGO composite powder

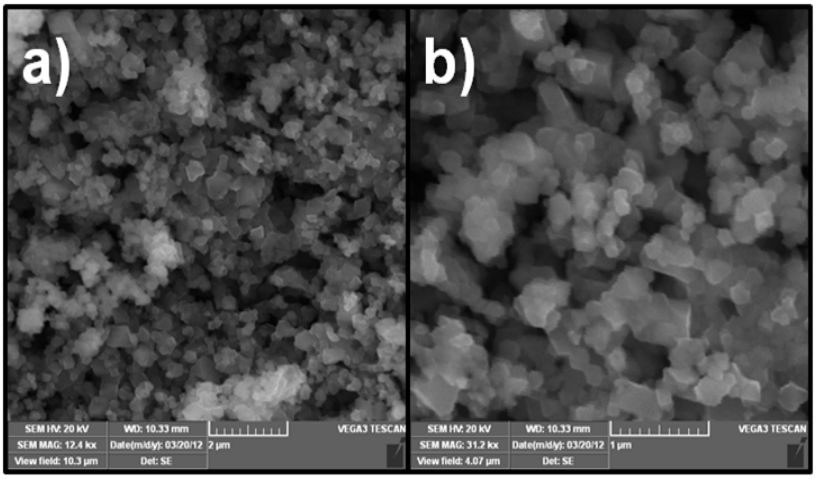

Fig. S3. SEM images of (a) Li_2FeSiO_4 and (b) Li_2MnSiO_4 samples synthesized by solvothermal process

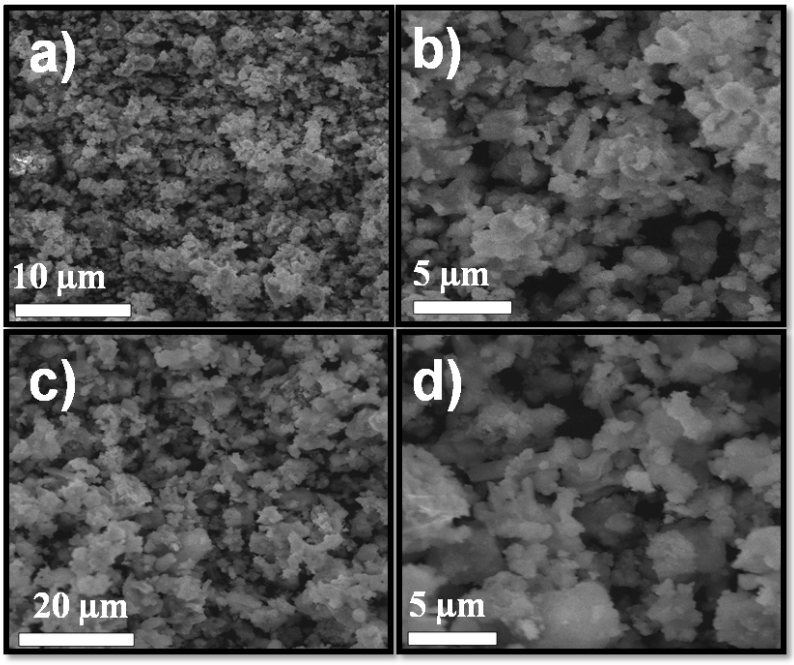

Fig. S4. SEM images of sol-gel derived (a-b) $Li_2FeSiO_4$and (c-d) Li_2MnSiO_4 synthesized at 700ºC

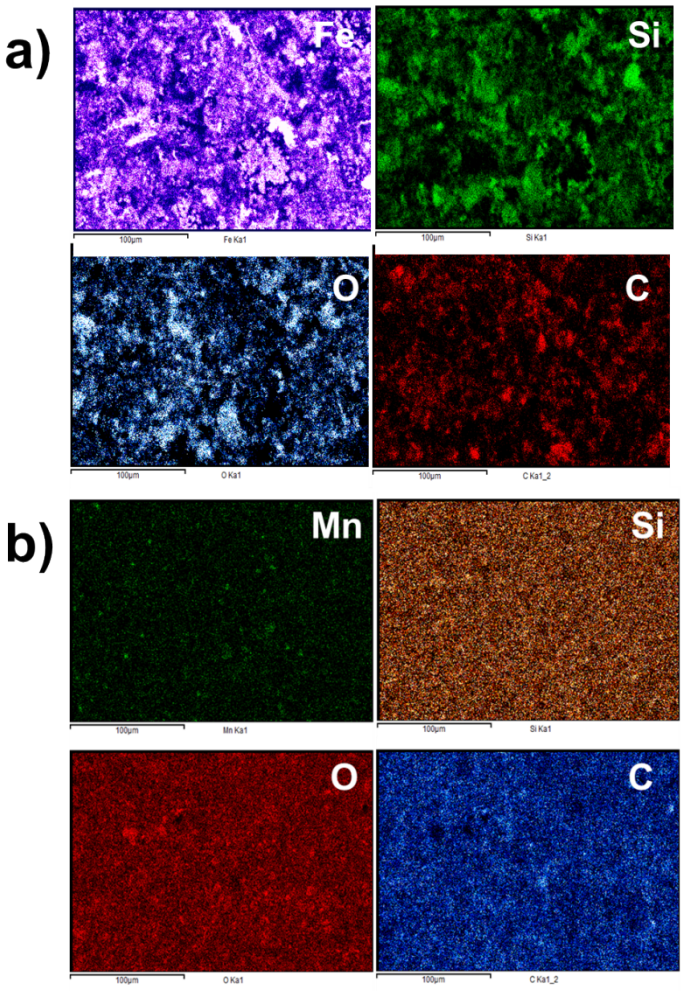

Fig. S5. Elemental mapping results of (a) Li_2FeSiO_4 (b) Li_2MnSiO_4 samples, indicating the homogeneous distribution of Fe/Mn, Si, and O atoms

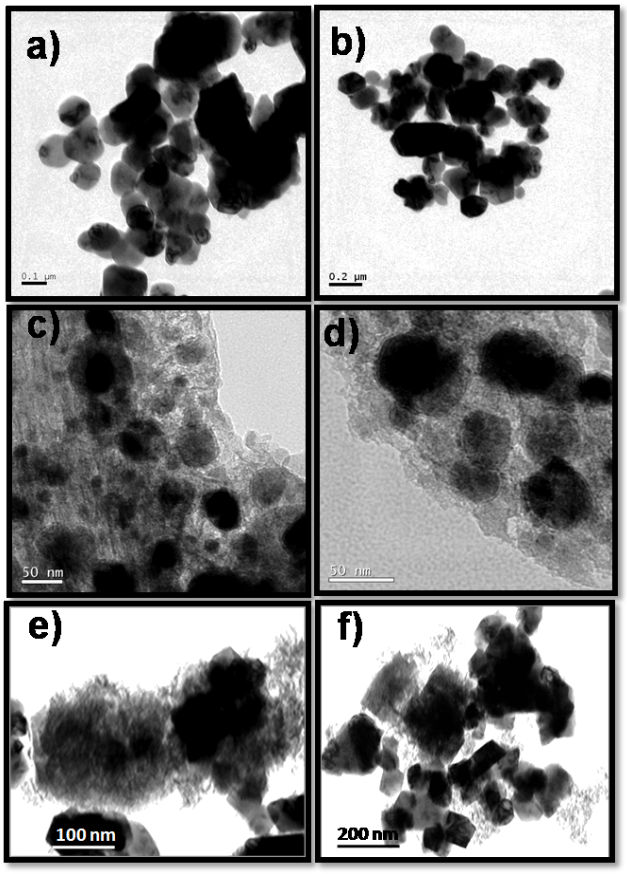

Fig. S6. TEM images of (a) Li_2FeSiO_4(b) Li_2MnSiO_4 samples synthesized by solvothermal process at 300^oC; (c-d) typical TEM images of Li_2MnSiO_4/C prepared by ball milling of orthosilicate active material with 10 wt% of super P carbon; (e-f) Typical TEM images of Li_2MnSiO_4/CNT composite

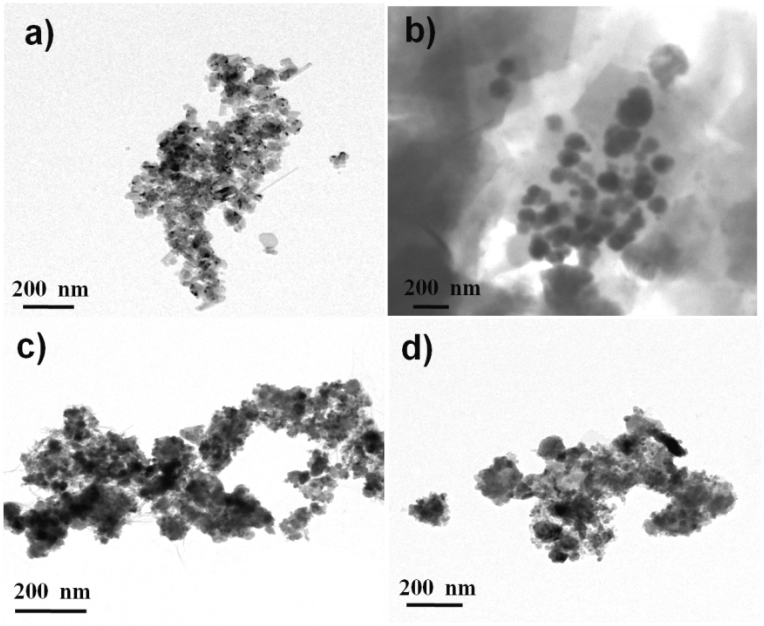

Fig. S7. TEM images of (a-b) Li_2FeSiO_4/rGO and (c-d) Li_2MnSiO_4/rGO composites

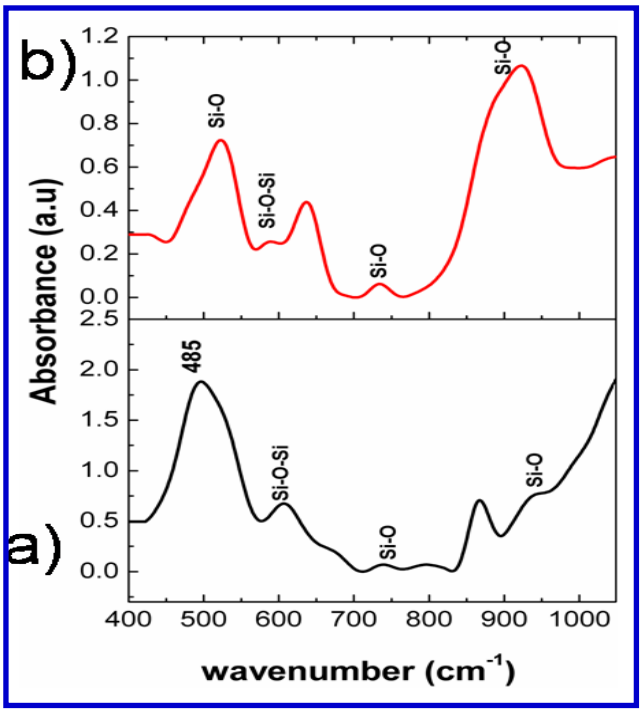

Fig. S8. FT-IR spectra of (a) Li_2FeSiO_4 and (b) Li_2MnSiO_4 samples

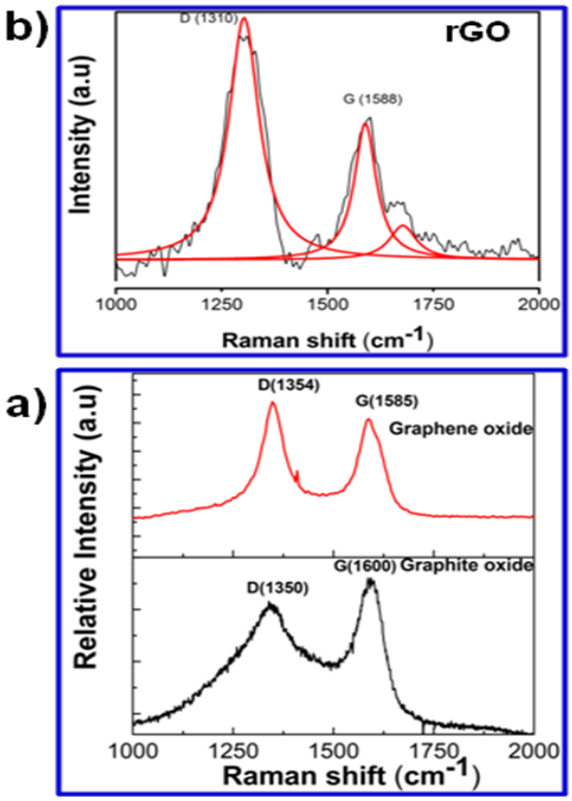

Fig. S9. (a) Raman spectrum of Graphite oxide and Graphene oxide synthesized by modified Hummer's method; (b) Reduced graphene oxide after the addition of hydrazine hydrate followed by thermal treatment

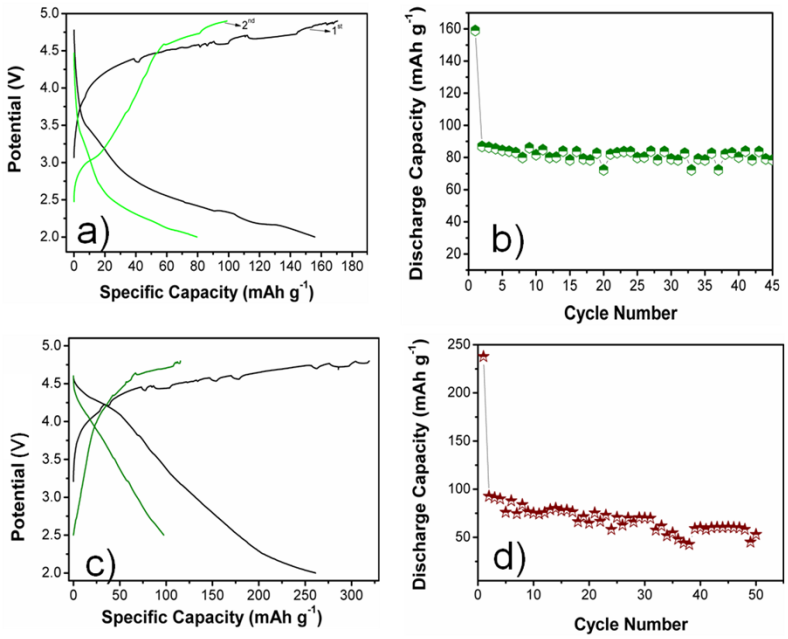

Fig. S10. Charge and discharge profile of first and second cycles and respective cycling performance of super P composite electrode measured at C/20 rate (a-b) Li_2FeSiO_4/C samples; (b) Li_2MnSiO_4/C sample

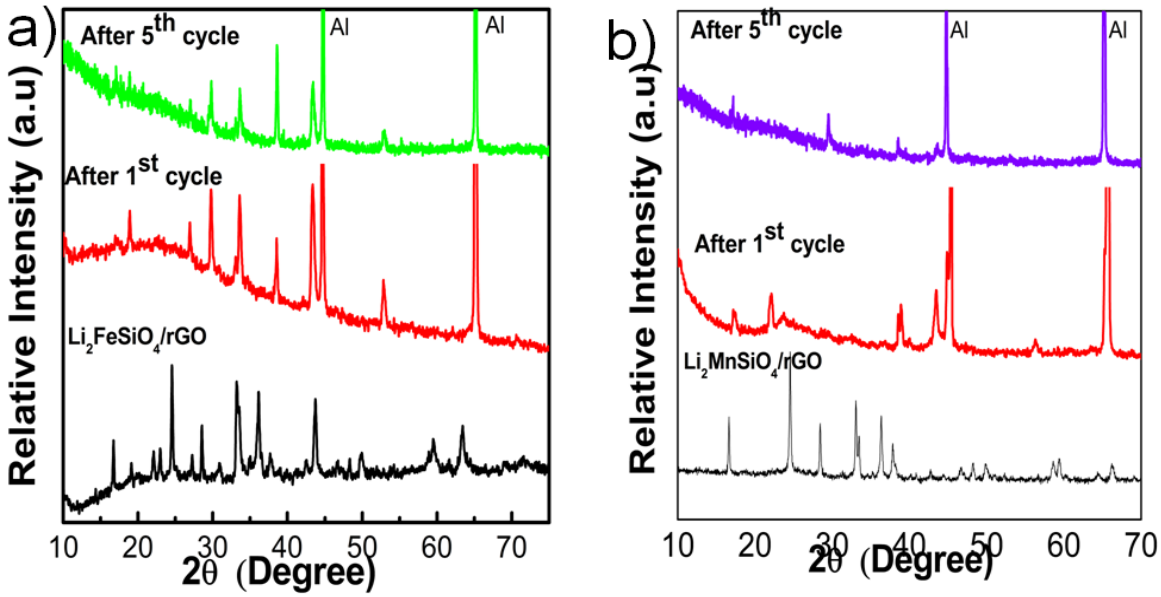

Fig. S11. Ex-situ XRD analysis during cycling of the Li_2FeSiO_4/rGO and Li_2MnSiO_4/rGO electrodes after cycling

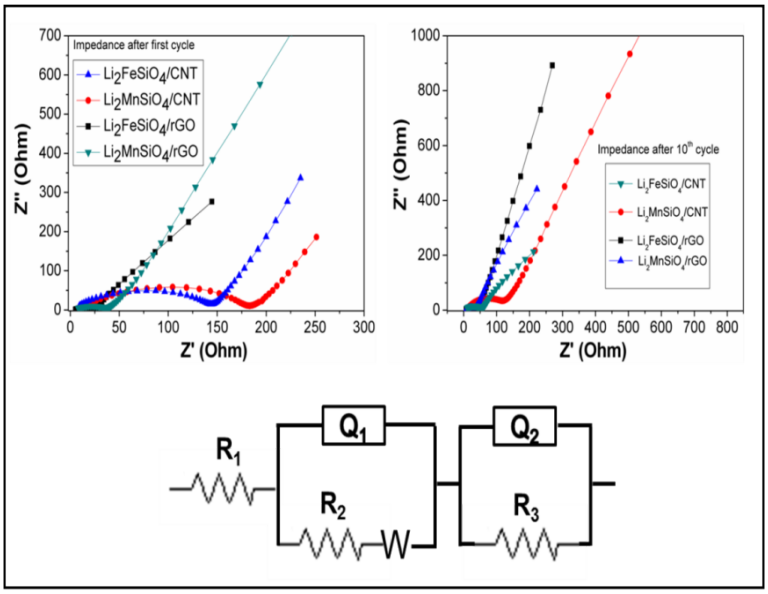

Fig. S12. Impedance behavior of individual electrodes at the first and 10th cycle

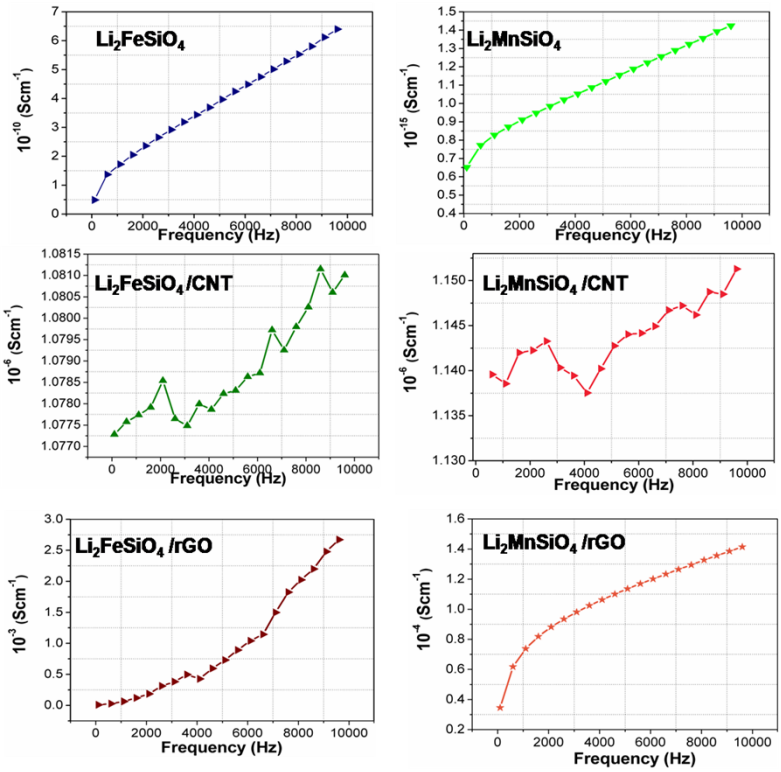

Fig. S13. Conductivity behavior of (a-b) bare Li_2MSiO_4 powder samples; (c-d) Li_2FeSiO_4/CNT and Li_2MnSiO_4/CNT composite; (e-f) Li_2FeSiO_4/rGO and Li_2MnSiO_4/rGO cathode